Nonequilibrium Transport in a Superfluid Josephson Junction Chain: Is There Negative Differential Conductivity?

Samuel E. Begg,[1,2,*] Matthew J. Davis,[2,†] and Matthew T. Reeves[2,‡]
[1]Asia Pacific Center for Theoretical Physics, Pohang 37673, Korea
[2]Australian Research Council Centre of Excellence in Future Low-Energy Electronics Technologies, School of Mathematics and Physics, University of Queensland, St. Lucia, Queensland 4072, Australia

(Received 27 July 2023; revised 10 December 2023; accepted 6 February 2024; published 7 March 2024)

We consider the far-from-equilibrium quantum transport dynamics in a 1D Josephson junction chain of multimode Bose-Einstein condensates. We develop a theoretical model to examine the experiment of Labouvie *et al.* [Phys. Rev. Lett. **115**, 050601 (2015)], wherein the phenomenon of negative differential conductivity (NDC) was reported in the refilling dynamics of an initially depleted site within the chain. We demonstrate that a unitary c-field description can quantitatively reproduce the experimental results over the full range of tunnel couplings, and requires no fitted parameters. With a view toward atomtronic implementations, we further demonstrate that the filling is strongly dependent on spatial phase variations stemming from quantum fluctuations. Our findings suggest that the interpretation of the device in terms of NDC is invalid outside of the weak coupling regime. Within this restricted regime, the device exhibits a hybrid behavior of NDC and the ac Josephson effect. A simplified circuit model of the device will require an approach tailored to atomtronics that incorporates quantum fluctuations.

DOI: 10.1103/PhysRevLett.132.103402

Introduction.—Experiments in ultracold atomic gases allow unprecedented control over the dynamics of quantum systems. Developments such as arbitrary potential generation [1] and single-site addressing schemes [2–4] have driven interest in the development of so-called "atomtronic" systems, consisting of circuits and devices that leverage quantum features such as coherence or superfluid transport [5–15]. Atomtronic simulators have also proven a powerful platform for probing a diverse range of nonequilibrium phenomena in quantum many-body systems within a simplified setting, for example, quench dynamics [16–19], universal scaling phenomena [20–23], and quantum turbulence [24–26].

Atomtronic systems utilizing optical lattice potentials are particularly suited for simulating nonequilibrium transport phenomena as occurs, for example, in the dynamics of Josephson junctions [10,27–29]. In a recent experiment, Labouvie *et al.* [27] studied a "multimode" Josephson array, formed by loading a large prolate atomic BEC into a 1D optical lattice. The resulting Josephson array, shown schematically in Fig. 1(a), consisted of a chain of quasi-2D Bose-Einstein condensates (BECs), harmonically confined radially in r, and coupled by nearest-neighbor hopping J along z. Using a site-selective electron beam, the experiment removed the atoms from the central site, and then observed the subsequent refilling dynamics [Fig. 1(b)].

The main finding of Ref. [27] was the observation of a novel current-filling relation in the central site. Unlike the ac oscillations characteristic of a standard (two-mode) Josephson junction, the system exhibited an emergent dc current; as shown schematically in Fig. 1(c), the atom current onto the central site, $I = dN_0/dt$, was Ohmic at small biases (Ω). Meanwhile, at large biases ($\mathcal{N}$), the junction exhibited the phenomenon of negative differential conductivity (NDC), wherein the current decreased with increasing "chemical voltage" $\Delta\mu$:

$$dI/d(\Delta\mu) < 0 \qquad \text{(NDC)}. \tag{1}$$

The emergent NDC was shown to be enabled by an atom-number-dependent effective tunneling rate J_{eff}, arising due

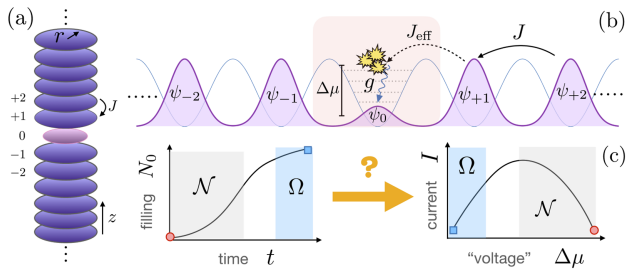

FIG. 1. (a) The multimode Josephson chain, considered experimentally in Ref. [27], consists of an array of pancake-shaped condensates. (b) The effective hopping rate J_{eff} onto the central depleted site is dependent on the atom number N_0, due to radial excitations; particles tunnel into radially excited modes and relax through the two-body interactions of strength g. (c) The atom number vs time (left panel) was found to exhibit a characteristic S shape. The inferred current-voltage relation (right panel) exhibited Ohmic behavior (Ω) at small biases, and negative differential conductivity ($\mathcal{N}$) at large biases.

to many radially excited modes altering the tunneling dynamics [Fig. 1(b)].

NDC is widely utilized in traditional semiconductor electronics [30], and has more recently been observed in systems such as molecular break junctions [31] and multilayer graphene [32]. The strongly non-Ohmic behavior of NDC thus presents interesting prospects for atomtronic systems; its characteristic multivalued current-voltage relation [cf. Fig. 1(c)] enables the construction of elements such as diodes, thyristors, and transistors [30]. Furthermore, the mechanisms leading to NDC are typically nonequilibrium ("hot-carrier") phenomena [33,34], and its observation in an atomtronic setting thus hints that additional far-from-equilibrium quantum transport scenarios may be realizable with ultracold atoms. This, in turn, might provide new insights into nonequilibrium quantum transport more generally, as ultracold atom systems offer a means to study phenomena difficult to probe in detail in the solid state [35,36]. While the average filling behavior observed experimentally has been reproduced by effective few-mode models [27,37], a more complete model of the many-body dynamics presents a considerable theoretical challenge, and, to date, this has precluded a comprehensive understanding of the atomtronic NDC mechanism.

In this Letter, we develop a numerically tractable model for the nonequilibrium transport dynamics in the multimode Josephson chain. In contrast to previous effective single-particle or few-mode approximations [27,37–39], we build a model within the framework of classical field theory which fully captures the many-body and multimode nature of the problem. Not only does our approach yield quantitative agreement with the experimental observations (without any fitted parameters), it further allows the underlying mechanisms of the reported NDC to be probed in detail. We are able to demonstrate that (i) the device current is in fact nowhere Ohmic, and that this apparent behavior is due to the probabilistic nature of the refilling seeded by quantum fluctuations; (ii) the interpretation of the current relation in terms of NDC is severely limited by the importance of phase dynamics and the far-from equilibrium nature of the system; and (iii) the device displays a combination of NDC- and ac Josephson-type behavior. An important implication of our results for atomtronics is that electronic analogs should be approached with caution, and that a tailored theoretical approach specific to atomtronic junctions is likely required.

Model.—We model the multimode junction using c-field theory, also known as the truncated Wigner approximation (TWA) [40–42]. Essentially, the TWA approximates the dynamics of the quantum system as a classical field (c-field), with quantum fluctuations accounted for at first order by adding a specified amount of noise to the initial conditions (for a review, see, e.g., Ref. [42]).

We describe the system on each site i using a stochastic classical field $\psi_i(\boldsymbol{x}, t)$. The fields evolve according to coupled Gross-Pitaevskii equations

$$i\hbar\partial_t\psi_i = \mathcal{L}\psi_i + J(\psi_{i-1} + \psi_{i+1}), \tag{2}$$

where

$$\mathcal{L}\psi_i = \mathcal{P}\left\{\left[-\frac{\hbar\nabla^2}{2m} + V(\boldsymbol{x}) + g_2|\psi_i|^2\right]\psi_i\right\}, \tag{3}$$

is the (projected) Gross-Pitaevski operator and $V(\boldsymbol{x}) = \frac{1}{2}m\omega_r^2(x^2+y^2)$ provides harmonic confinement in the x-y plane with frequency ω_r. The interaction strength is $g_2 = g\int dz|w(z)|^4$, where $w(z)$ is the Wannier function associated with the optical lattice in the z direction and $g = 4\pi\hbar^2 a_s/m$, with s-wave scattering length a_s. The tunneling rate J is determined by diagonalizing the optical lattice Hamiltonian (in the z direction), $\hat{H} = -\hbar^2\partial_z^2/2m + V_0\sin^2(2\pi z/\lambda)$, and using a tight-binding approximation (see Supplemental Material [43]). The projector $\mathcal{P}$ limits the dynamics of Eq. (2) to the single particle modes that are highly occupied (i.e., the classical field region) via an energy cutoff [43]. Provided this is appropriately chosen, the model is insensitive to its precise value; we emphasise this leaves no free parameters in the model.

Tunneling between neighboring sites i and $j = i \pm 1$ depends on the overlap between the respective fields. This is evidenced through the evolution of the atom number on site i, N_i,

$$\frac{dN_i}{dt} = \frac{2J}{\hbar}\left(\eta_{i+1,i}\sqrt{N_{i+1}N_i} + \eta_{i-1,i}\sqrt{N_{i-1}N_i}\right), \tag{4}$$

with the "Frank-Condon factors"

$$\begin{aligned}\eta_{i,j}(t) &= \mathrm{Im}[\langle\psi_i|\psi_j\rangle]/\sqrt{N_i N_j}, \\ &= \frac{1}{\sqrt{N_i N_j}}\int d^2\boldsymbol{x}\sqrt{n_i(\boldsymbol{x})n_j(\boldsymbol{x})}\,\sin[\varphi_{ij}(\boldsymbol{x})],\end{aligned} \tag{5}$$

where $\psi_i(\boldsymbol{x}) = \sqrt{n_i(\boldsymbol{x})}e^{i\phi_i(\boldsymbol{x})}$ and $\varphi_{ij}(\boldsymbol{x}) \equiv \phi_i(\boldsymbol{x}) - \phi_j(\boldsymbol{x})$. The number-dependent filling mechanism is thus explicitly contained within the c-field formalism; this contrasts with the effective single particle description employed in Ref. [27], where it was assumed to be $\eta_{i,j} \sim |\langle\psi_i|\psi_j\rangle|$, and approximated *a posteriori* to be linear in the particle difference $|N_i - N_j|$.

Results.—We solve Eq. (2) via a pseudospectral method with quadrature using XMDS2 [49], enabling accurate simulation of a large number of sites. Throughout we work in radial harmonic oscillator units, giving units for energy $\hbar\omega_r$, length $l_r = \sqrt{\hbar/m\omega_r}$, and time ω_r^{-1}. We model the experiment using a uniform 21-site chain; each site (for $i \neq 0$) contains $N_f \sim 700$ atoms [27], and $g_2 \sim 0.2\hbar\omega l_r^2$, giving $\mu_R \sim 7\hbar\omega_r$. As per Ref. [27], the central site ($i = 0$) is populated such that the atom number is $N_0/N_f \sim 5\%$.

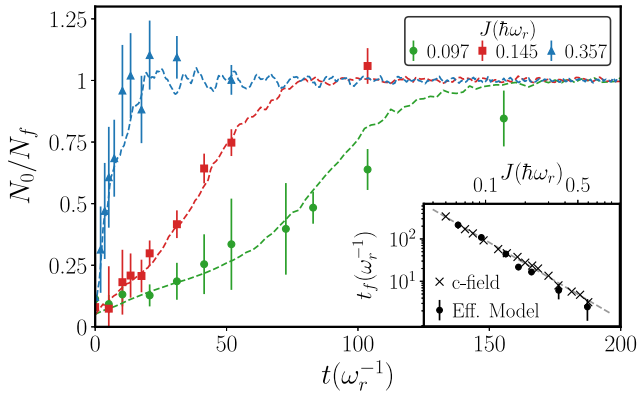

FIG. 2. Atom number N_0/N_f vs time for different tunnel couplings J, comparing results obtained via 100 trajectories of the c-field model (2) (dashed lines) with the experimental data of Ref. [27] (points). Inset: Log-log plot of fill times t_f vs J as predicted by the c-field model (crosses) and the fitted effective single particle model presented in Ref. [27] (dots). Dashed line shows a fit to the simulation data $t_f \propto J^{-\alpha}$ with $\alpha = 1.82(3)$.

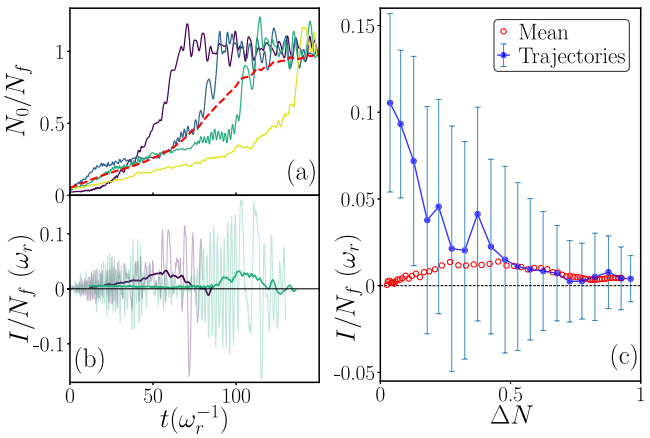

FIG. 3. (a) Comparison of the atom number N_0/N_f vs time for five individual trajectories (solid lines), compared with the mean of 100 trajectories (dashed line) with $J/\hbar\omega_r = 0.097$ [50]. (b) Normalized particle current into the central site I vs time for two trajectories (light lines). The dark lines show the corresponding rolling averages. (c) I vs atom number difference (normalized) $\Delta N = (N_f - N_0)/N_f$, comparing the rate of change of the mean atom number $I_m = d\langle N_0\rangle/dt$ (circles), against the average trajectory current $I_t = \langle dN_0/dt\rangle$ (dots). Error bars show the standard deviation [51].

From a detailed modeling of the experimental preparation protocol, we find that, at the end of the preparation sequence, the left and right chains become nearly uncorrelated in their phases. For the initial conditions, we therefore multiply one of the chains by a random phase to mimic this phase diffusion. Full details of the experimental modeling setup and simulation method are provided in Supplemental Material [43].

We first compare the results of the numerical simulations directly against the experimental observations of Ref. [27]. In Fig. 2 we show the atom number N_0/N_f vs time for three different tunneling couplings J. The c-field model is in excellent agreement across the full range of coupling values. The model produces the characteristic S-shaped filling curves, which suggest Ohmic behavior at small voltages (late times) and NDC at large voltages (early times) [cf. Fig. 1(c)]. Figure 2 (inset) shows the filling time t_f defined as the time at which N_0 reaches $2/3$ of its final value [27]. We find the filling time obeys the power law $t_f \propto J^{-\alpha}$, with $\alpha = 1.82(3)$. This is in good agreement with the value of $\alpha = 1.9(1)$ obtained in Ref. [27] which utilized an effective single particle model with a fitted decoherence parameter.

Having established that the model quantitatively reproduces experimental observations, we now turn to gaining deeper insight into the mechanisms underlying the NDC-type behavior. The experimental measurement protocol of Labouvie *et al.* [27] was destructive, so that every data point in Fig. 2(a) is an average over several experimental runs beginning with an independent condensate. Consequently, the results of single experiments cannot be inferred. However, for the TWA, the individual simulation trajectories approximately correspond to the behavior of single experimental runs [42]. In Fig. 3(a) we compare the mean atom number vs time, $\langle N_0(t)\rangle$ (red-dashed line), with $N_0(t)$ for several individual simulation trajectories, with $J/\hbar\omega_r = 0.097$ [50].

In the simulations the individual trajectories and overall curve for the mean $\langle N_0(t)\rangle$ exhibit similar behavior at early times but markedly different behavior at late times. In particular, the characteristic S shape that was observed experimentally [cf. Fig. 2] only appears in the mean of the simulation data; it emerges due to the probabilistic filling of the individual trajectories, which have different filling times due to quantum noise. In individual trajectories [Fig. 3(a)], the current can be seen to in fact *accelerate* rather than decelerate during the latter stages of filling. Unlike the smooth growth of the mean, the current in individual trajectories is a rapidly oscillating chirped signal in time [Fig. 3(b)]. In many trajectories a rapid growth of the atom number occurs during latter stages of the filling [Fig. 3(a)]; this is accompanied by oscillations that increase in amplitude and decrease in frequency as time progresses. This rapid growth phase also coincides with a sudden growth in the condensate fraction [43]; the late-stage oscillations are thus strongly suggestive of the "ac Josephson effect" previously observed in, for example, Refs. [52,53].

Differences between the mean and individual trajectories are further highlighted in Fig. 3(c), which shows the rate of change of the mean atom number $I_m = d\langle N_0\rangle/dt$ and the average trajectory current $I_t = \langle dN_0/dt\rangle$, plotted against the atom number difference $\Delta N = (N_f - N_0)/N_f$. For $\Delta N \gtrsim 0.6$ ($t \lesssim t_f$), we find $I_t \approx I_m$, with both exhibiting the NDC characteristic Eq. (1). However, for $\Delta N \lesssim 0.6$ ($t \gtrsim t_f$), we find $I_t \neq I_m$. Notably, the Ohmic region

($I \propto \Delta N$) seen in I_m is only apparent in the average. Contrarily, the trajectory data in Fig. 3(c) suggest that the individual trajectories instead exhibit the NDC characteristic over the entire range of ΔN. The rapid current oscillations in the trajectories [Fig. 3(b)] also result in significant fluctuations in I_t [Fig. 3(c), error bars]; these are in fact larger than the average currents for most values of ΔN. Note that we have refrained from defining a "chemical voltage" $\Delta\mu$ as in Ref. [27], because this requires the assumption of quasiequilibrium, whereas ΔN is always defined. To support this, in Supplemental Material [43] we demonstrate that the experiment [27] is far from equilibrium.

The results in Fig. 3(a) show that the trajectories certainly exhibit the NDC characteristic Eq. (1). However, this alone is not sufficient for the behavior to be classified as NDC; it is also necessary to consider the role played by the relative phases between sites. NDC in the usual sense would require that the phase information is unimportant, such that the current can be characterized simply through the particle number difference as $I = I(\Delta N)$. By contrast, Josephson junctions are characterized by both an imbalance (voltage) and their intrinsic phase difference, i.e., $I = I(\Delta N, \varphi)$, and for this reason they are not readily classified as NDC elements despite exhibiting quasi-NDC-type behavior [30,54].

To investigate the role of the phase in the dynamics, we consider the phase difference between the nearest-neighbor sites $i = \pm 1$ in individual trajectories. We define $\Delta\Phi_i = \Phi_{i+1} - \Phi_{i-1}$, where Φ_i is the spatially averaged phase $\Phi_i = \mathcal{A}^{-1}\int_{\mathcal{A}} d^2\boldsymbol{x}\phi_i \equiv \langle\phi_i\rangle_{\boldsymbol{x}}$ (where $\mathcal{A}$ is a central region in well i). Figure 4 shows the dependence of the filling dynamics on the initial phase difference across the central site, $\Delta\Phi_0$, for three different values of J. For small couplings ($J/\hbar\omega_r = 0.05$), the filling time is found to be approximately independent of the initial phase difference. However, for moderate tunneling ($J/\hbar\omega_r = 0.2$), when the left and right chains are initially out of phase ($|\Delta\Phi_0| \sim \pi$) the filling time is approximately double that of the synchronized case $|\Delta\Phi_0| \sim 0$. For large couplings ($J/\hbar\omega_r = 0.6$),

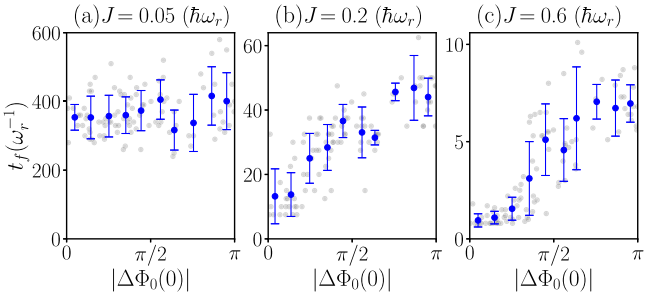

FIG. 4. Influence of the initial phase on the filling dynamics. (a) Filling time t_f vs initial phase difference $|\Delta\Phi_0(0)|$ for different tunneling strengths J. Light markers show individual trajectories, dark markers with error bars show average and standard deviation (obtained by histogramming over 10 bins in the range $|\Delta\Phi_0| \in [0, \pi]$).

this discrepancy becomes even larger, yielding a factor of ~6 difference in the filling times between the zero-phase and π-phase difference scenarios. For $|\Delta\Phi_0| \sim \pi$, we also observe a significant increase in the fluctuations of the filling time, as seen in the large standard deviations indicated by the error bars.

Discussion.—Our results suggest that the NDC interpretation put forward in Ref. [27] is only valid at small values of J and during the early stages of the filling dynamics, where phase coherence is unimportant. For most regimes the phase difference is a crucial element in the dynamics. Indeed, Eq. (4) shows that both the particle number difference and phase differences drive the current, since $\eta_{i,j} \propto \Im\{\langle\psi_i|\psi_j\rangle\}$ rather than $|\langle\psi_i|\psi_j\rangle|$ as was assumed in Ref. [27]. To consider the average contributions from the phase, one should consider the conjugate equation to Eq. (4), which governs the evolution of the spatially averaged phase Φ_j:

$$\hbar\partial_t\Phi_j + \mu_j^{\mathrm{eff}} = J\zeta_j, \tag{6}$$

with

$$\mu_j^{\mathrm{eff}} = \left\langle \frac{1}{2}m\mathbf{u}_j^2 + g_2 n_j + V - \frac{\hbar^2}{2m}\frac{\nabla^2\sqrt{n_j}}{\sqrt{n_j}} \right\rangle_{\boldsymbol{x}}, \tag{7}$$

where $\mathbf{u}_j(\boldsymbol{x}, t) = \hbar\nabla\phi_j(\boldsymbol{x}, t)/m$ is the velocity field on site j, and

$$\zeta_j = \left\langle \sqrt{\frac{n_{j+1}}{n_j}}\cos(\varphi_{j+1,j}) + \sqrt{\frac{n_{j-1}}{n_j}}\cos(\varphi_{j-1,j}) \right\rangle_{\boldsymbol{x}}. \tag{8}$$

The evolution of the average variables (N_j, Φ_j) relies on a rather nontrivial coarse graining over the internal dynamics of the sites; this depends on the instantaneous density fields n_j, relative phases φ_{ij}, and on-site velocity fields $\mathbf{u}_j$.

Our model clearly reproduces the observed experimental behavior, and thus serves as a natural starting point for developing a reduced "lumped-element"-type description. However, whether the full dynamics of Eq. (2) can indeed be reduced to a simple effective model in terms of (N_j, Φ_j) remains an open problem. We anticipate the results could be significantly affected by, e.g., thermal effects (condensate fraction), collective modes, or quantized vortices, which all affect the average phase coherence. While a comprehensive study of finite temperature effects is beyond the scope of the present work, we performed simulations of a mostly incoherent process (< 5% condensate fraction in the reservoirs), which further support the interpretations put forward here (see [43]). In particular, the acceleration of the current in individual trajectories is absent for the incoherent filling process, indicating that phase coherence is essential for this process to occur. Finally, we note that many of the system's qualitative dynamical features can be reproduced

by a simple "coherent reservoir" model, wherein the reservoir is treated as a coherent ac drive. This model was described in Ref. [55] to model a related experiment wherein dissipation was introduced to the central site [28], and may serve as a useful starting point for a simplified description of multimode Josephson junction dynamics.

Conclusions.—We have characterized the nonequilibrium dynamics of a many-body, multimode bosonic Josephson chain, and demonstrated that a c-field description can quantitatively reproduce the observations of Ref. [27] with no fitted parameters. Our model suggests that the dynamics are strongly dependent on both the atom number and phase. We argue this makes the NDC interpretation invalid for the majority of the couplings considered in Ref. [27]. The filling appears to be a "two-stage" process: our results do suggest that the NDC interpretation is valid at small J and during the initial (gradual) phase of the filling, before phase coherence is established. However, this interpretation is complicated in latter (rapid) stages of the filling by the emergence of phase coherence and strong Josephson oscillations. Additionally, significant (quantum) fluctuations are present, and will likely need to be incorporated into any simplified effective model that quantitatively reproduces the salient features of the dynamics. From a device perspective, it would be worthwhile considering how the atomtronic junction behaves under an enforced chemical potential bias, rather than under free dynamics, so as to be considered as a single component of a larger dc or ac atomtronic circuit.

We acknowledge useful discussions with H. Ott and A. S. Bradley. This research was partially supported by the Australian Research Council Centre of Excellence in Future Low-Energy Electronics Technologies (FLEET, Project No. CE170100039) and funded by the Australian Government. M. T. R. is supported by an Australian Research Council Discovery Early Career Researcher Award (DECRA), Project No. DE220101548. S. E. B. acknowledges the support of the Young Scientist Training Program at the Asia Pacific Center for Theoretical Physics.

*samuel.begg@apctp.org
†mdavis@uq.edu.au
‡m.reeves@uq.edu.au

[1] G. Gauthier, I. Lenton, N. M. Parry, M. Baker, M. J. Davis, H. Rubinsztein-Dunlop, and T. W. Neely, Optica **3**, 1136 (2016).
[2] W. S. Bakr, J. I. Gillen, A. Peng, S. Fölling, and M. Greiner, Nature (London) **462**, 74 (2009).
[3] P. Würtz, T. Langen, T. Gericke, A. Koglbauer, and H. Ott, Phys. Rev. Lett. **103**, 080404 (2009).
[4] G. J. A. Edge, R. Anderson, D. Jervis, D. C. McKay, R. Day, S. Trotzky, and J. H. Thywissen, Phys. Rev. A **92**, 063406 (2015).
[5] B. T. Seaman, M. Krämer, D. Z. Anderson, and M. J. Holland, Phys. Rev. A **75**, 023615 (2007).
[6] S. Eckel, J. G. Lee, F. Jendrzejewski, N. Murray, C. W. Clark, C. J. Lobb, W. D. Phillips, M. Edwards, and G. K. Campbell, Nature (London) **506**, 200 (2014).
[7] M. K. Olsen and A. S. Bradley, Phys. Rev. A **91**, 043635 (2015).
[8] G. Kordas, D. Witthaut, and S. Wimberger, Ann. Phys. (Amsterdam) **527**, 619 (2015).
[9] S. C. Caliga, C. J. E. Straatsma, and D. Z. Anderson, New J. Phys. **19**, 013036 (2017).
[10] A. Burchianti, F. Scazza, A. Amico, G. Valtolina, J. A. Seman, C. Fort, M. Zaccanti, M. Inguscio, and G. Roati, Phys. Rev. Lett. **120**, 025302 (2018).
[11] C. Ryu, E. Samson, and M. G. Boshier, Nat. Commun. **11**, 3338 (2020).
[12] L. Amico, M. Boshier, G. Birkl, A. Minguzzi, C. Miniatura, L.-C. Kwek, D. Aghamalyan, V. Ahufinger, D. Anderson, N. Andrei *et al.*, AVS Quantum Sci. **3**, 039201 (2021).
[13] S. Pandey, H. Mas, G. Vasilakis, and W. von Klitzing, Phys. Rev. Lett. **126**, 170402 (2021).
[14] A. Pérez-Obiol, J. Polo, and L. Amico, Phys. Rev. Res. **4**, L022038 (2022).
[15] D. S. Grün, L. H. Ymai, K. W. W, A. P. Tonel, A. Foerster, and J. Links, Phys. Rev. Lett. **129**, 020401 (2022).
[16] T. Kinoshita, T. Wenger, and D. S. Weiss, Nature (London) **440**, 900 (2006).
[17] C.-L. Hung, V. Gurarie, and C. Chin, Science **341**, 1213 (2013).
[18] M. Pigneur, T. Berrada, M. Bonneau, T. Schumm, E. Demler, and J. Schmiedmayer, Phys. Rev. Lett. **120**, 173601 (2018).
[19] Z. Chen, T. Tang, J. Austin, Z. Shaw, L. Zhao, and Y. Liu, Phys. Rev. Lett. **123**, 113002 (2019).
[20] G. Lamporesi, S. Donadello, S. Serafini, F. Dalfovo, and G. Ferrari, Nat. Phys. **9**, 656 (2013).
[21] S. Krinner, D. Stadler, D. Husmann, J.-P. Brantut, and T. Esslinger, Nature (London) **517**, 64 (2015).
[22] S. Erne, R. Bücker, T. Gasenzer, J. Berges, and J. Schmiedmayer, Nature (London) **563**, 225 (2018).
[23] C. Eigen, J. A. Glidden, R. Lopes, E. A. Cornell, R. P. Smith, and Z. Hadzibabic, Nature (London) **563**, 221 (2018).
[24] N. Navon, A. L. Gaunt, R. P. Smith, and Z. Hadzibabic, Nature (London) **539**, 72 (2016).
[25] N. Navon, C. Eigen, J. Zhang, R. Lopes, A. L. Gaunt, K. Fujimoto, M. Tsubota, R. P. Smith, and Z. Hadzibabic, Science **366**, 382 (2019).
[26] M. T. Reeves, K. Goddard-Lee, G. Gauthier, O. R. Stockdale, H. Salman, T. Edmonds, X. Yu, A. S. Bradley, M. Baker, H. Rubinsztein-Dunlop *et al.*, Phys. Rev. X **12**, 011031 (2022).
[27] R. Labouvie, B. Santra, S. Heun, S. Wimberger, and H. Ott, Phys. Rev. Lett. **115**, 050601 (2015).
[28] R. Labouvie, B. Santra, S. Heun, and H. Ott, Phys. Rev. Lett. **116**, 235302 (2016).
[29] R. Ceulemans and M. Wouters, Phys. Rev. A **108**, 013314 (2023).
[30] M. P. Shaw, V. V. Mitin, E. Schöll, and H. L. Grubin, Introduction, in *The Physics of Instabilities in Solid State*

Electron Devices, edited by M. P. Shaw, V. V. Mitin, E. Schöll, and H. L. Grubin (Springer US, Boston, MA, 1992), pp. 1–70.
[31] M. L. Perrin, R. Frisenda, M. Koole, J. S. Seldenthuis, J. A. C. Gil, H. Valkenier, J. C. Hummelen, N. Renaud, F. C. Grozema, J. M. Thijssen *et al.*, Nat. Nanotechnol. **9**, 830 (2014).
[32] L. Britnell, R. Gorbachev, A. Geim, L. Ponomarenko, A. Mishchenko, M. Greenaway, T. Fromhold, K. Novoselov, and L. Eaves, Nat. Commun. **4**, 1794 (2013).
[33] A. F. Volkov and S. M. Kogan, Sov. Phys. Usp. **11**, 881 (1969).
[34] B. R. Pamplin, Contemp. Phys. **11**, 1 (1970).
[35] J.-P. Brantut, C. Grenier, J. Meineke, D. Stadler, S. Krinner, C. Kollath, T. Esslinger, and A. Georges, Science **342**, 713 (2013).
[36] C.-C. Chien, S. Peotta, and M. Di Ventra, Nat. Phys. **11**, 998 (2015).
[37] C. Mink, A. Pelster, J. Benary, H. Ott, and M. Fleischhauer, SciPost Phys. **12**, 051 (2022).
[38] M. K. Olsen and J. F. Corney, Phys. Rev. A **94**, 033605 (2016).
[39] D. Fischer and S. Wimberger, Ann. Phys. (Amsterdam) **529**, 1600327 (2017).
[40] M. J. Steel, M. K. Olsen, L. I. Plimak, P. D. Drummond, S. M. Tan, M. J. Collett, D. F. Walls, and R. Graham, Phys. Rev. A **58**, 4824 (1998).
[41] A. Polkovnikov, Phys. Rev. A **68**, 053604 (2003).
[42] P. B. Blakie, A. S. Bradley, M. J. Davis, R. J. Ballagh, and C. W. Gardiner, Adv. Phys. **57**, 363 (2008).
[43] See Supplemental Material at http://link.aps.org/supplemental/10.1103/PhysRevLett.132.103402 for full details of the simulation parameters, a discussion and demonstration of the robustness of the solutions to the initial conditions, an analysis of the condensation dynamics of the central site, and a numerical experiment demonstrating that the system is far from equilibrium. It also includes Refs. [44–48].
[44] R. Labouvie, Non-equilibrium dynamics in ultracold quantum gases with localized dissipation, Ph.D. thesis, Technischen Universität Kaiserslautern, 2015.
[45] J. P. Boyd, *Chebyshev and Fourier spectral methods* (Dover Publications, New York, 2001).
[46] M. Arzamasovs and B. Liu, Eur. J. Phys. **38**, 065405 (2017).
[47] W. Zwerger, J. Opt. B **5**, S9 (2003).
[48] A. Sinatra and Y. Castin, Phys. Rev. A **78**, 053615 (2008).
[49] G. R. Dennis, J. J. Hope, and M. T. Johnsson, Comput. Phys. Commun. **184**, 201 (2013).
[50] In order to sensibly compare the atom number for individual trajectories of the truncated Wigner approximation to the mean atom number, it is necessary to subtract half an atom per mode from the normalization of the trajectory in order to account for the initial quantum noise.
[51] To compensate for the disproportionate effect of small sampling errors in the region $N_0 \lesssim N_f$, for I_m we perform a rolling average over a time of $\Delta t = 10\omega_r^{-1}$. In (b), the rolling average is conducted over a window of $25\omega_r^{-1}$.
[52] S. V. Pereverzev, A. Loshak, S. Backhaus, J. C. Davis, and R. E. Packard, Nature (London) **388**, 449 (1997).
[53] S. Levy, E. Lahoud, I. Shomroni, and J. Steinhauer, Nature (London) **449**, 579 (2007).
[54] M. P. Shaw, V. V. Mitin, E. Schöll, and H. L. Grubin, Superconducting junctions, in *The Physics of Instabilities in Solid State Electron Devices*, edited by M. P. Shaw, V. V. Mitin, E. Schöll, and H. L. Grubin (Springer US, Boston, MA, 1992), pp. 325–358.
[55] M. T. Reeves and M. J. Davis, SciPost Phys. **15**, 068 (2023).